

The Effect of Hydrostatic Pressure on the Shear Yield Behaviour of Polymers

S. RABINOWITZ,* I. M. WARD†

H. H. Wills Physics Laboratory, University of Bristol, Bristol, UK

J. S. C. PARRY

Department of Mechanical Engineering, University of Bristol, Bristol, UK

The torsional stress-strain behaviour of isotropic poly(methylmethacrylate) (P M M A), poly(ethylene terephthalate) (P E T) and polyethylene has been studied under hydrostatic pressures up to 7 kbar.‡ In P M M A the following important features were observed. First, there is a monotonic increase in the initial slope of the stress-strain curve with increasing pressure. Secondly, there is a substantial increase in the yield stress and the strain to yield as pressure is raised. Thirdly, there is a transition in the mode of failure at elevated pressure, the specimens fracturing in the high pressure region before a drop in stress occurs. Finally, in the high pressure region the fracture stress increases with increasing pressure but the strain at fracture decreases.

The observed yield behaviour can be represented formally in a number of ways, and the results will therefore be discussed accordingly, in an attempt to give a general yield criterion for P M M A. The fracture behaviour has been analysed in terms of the Griffith ideas for fracture of glassy materials, and this will also be discussed.

The results for poly(ethylene terephthalate) (Arnite) differ significantly from those for P M M A. Specimens of Arnite as received from the manufacturers were ductile in torsion at atmospheric pressure, and the torsional yield stress rose monotonically with increasing hydrostatic pressure. Annealing the specimens produced embrittlement at atmospheric pressure, but on testing under conditions where there is no tensile component of stress (i.e. at very low hydrostatic pressures) ductile behaviour was observed.

The contrast between P M M A and Arnite suggests that in the former case there are *surface* flaws which are penetrated by the hydraulic fluid at high pressures, whereas in the latter case *internal* flaws are produced by annealing.

Polyethylene remained ductile over the complete pressure range, with a pressure dependence of the tensile yield stress which was similar to that shown by polyethylene terephthalate.

1. Introduction

A number of recent publications [1-6] have emphasised that the mechanical properties of several polymers are strongly dependent on the hydrostatic component of stress. Increases in both the stiffness and yield stress with increasing pressure have been observed in poly(methyl-

methacrylate) [1, 3], polypropylene [4], polystyrene [5], and a variety of other polymer systems [1, 6]. In addition, an increase in the fracture stress and strain with increasing hydrostatic stress has been reported for poly(methylmethacrylate) [1] and polystyrene [1, 6, 7] in uniaxial tension and compression. Brittle-

*Present address: Metallurgy Department, Scientific Research Staff, Ford Motor Company, PO Box 2053, Dearborn, Michigan, USA.

†Address from 1.1.70: Department of Physics, University of Leeds, Leeds, England.

‡1 bar = 10^5 N/m²

ductile transitions and changes in the nature of the fracture process have also been observed at high pressures [4, 7].

The variation of yield stress with pressure has been represented mostly in terms of the Coulomb yield criterion, where the critical resolved shear stress for yield is modified linearly by the normal stress acting on the yield plane. Fracture has generally been discussed in qualitative terms, it being difficult to evaluate the state of stress and strain beyond the yield point in specimens in which yield is accompanied by geometrical changes.

While the study of the mechanical behaviour of polymers under high hydrostatic pressure is still at an early stage in its development, sufficient evidence has been gathered to establish that any general theory of yield or fracture must incorporate a significant pressure dependence. Accordingly, a great deal of detailed information is required concerning the stress-strain behaviour of polymers subjected to a variety of combinations of stress. This paper is part of an extensive study of yield and fracture in isotropic and oriented polymers. Previous publications have dealt with the nature of the load drop at yield [8], the yield behaviour of oriented poly(ethylene terephthalate) [9], and the yield and fracture of isotropic poly(ethylene terephthalate) [10]. The present investigation was undertaken to study the torsional stress-strain response of isotropic poly(methylmethacrylate) (PMMA), poly(ethylene terephthalate) (PET), and polyethylene,

under hydrostatic pressures up to 7 kbar. The torsion experiment is particularly well suited to studies of yield and fracture since the state of stress in the test specimen remains well-defined over the entire stress-strain experiment.

2. Experimental

The apparatus for carrying out a torsion test on a specimen whilst it is completely surrounded by high pressure fluid was based on equipment originally described by Crossland [11] which was designed for a maximum pressure of 3 kbar.

The pressure vessel of the equipment used for these experiments which is shown in fig. 1 was designed for a pressure of 7 kbar by Kaye and Roberts [12].

The hollow specimen (L) is held in special torsion grips (C) similar to those originally designed by Professor J. L. M. Morrison and described by Crossland [11]. These grips, which are shown in detail in fig. 2, are designed so that only a pure torque can be transmitted to the specimen. The only possible axial constraint is due to the sliding friction of the balls on the hardened steel pads and this has been shown to be insignificant. One set of grips is attached to the torque tube (H) and the other through an extension piece (M) to the shaft (Q). A chain drive to the sprocket (S) rotates the shaft and thus twists the specimen. The torque reaction is taken by the torque tube, the elastic twist of which is measured by the relative rotation of the two mirrors (E). One mirror is attached to the

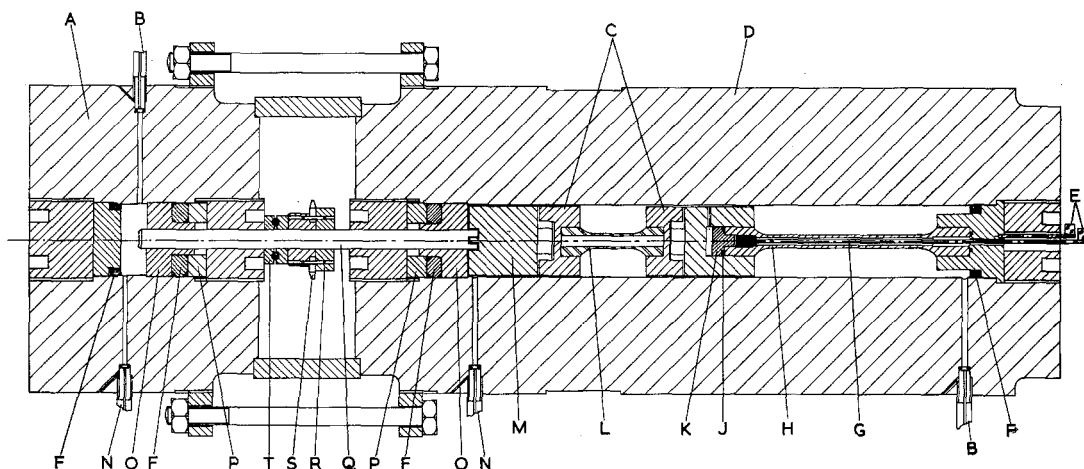


Figure 1 High pressure torsion testing apparatus: A, equalising pressure vessel; B, air outlet; C, torsion grips; D, main pressure vessel; E, mirrors; F, neoprene packing ring; G, mirror stalk; H, torque tube; J, "O" ring; K, plug; L, specimen; M, extension piece; N, oil inlet; O, Morrison seal; P, backing ring; Q, shaft; R, clamp; S, chain sprocket; T, thrust race.

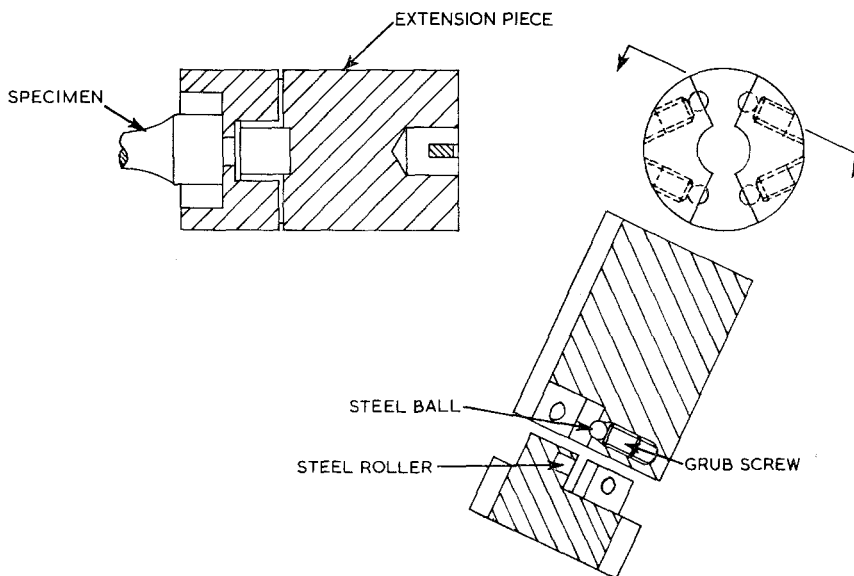


Figure 2 Details of torsion grips.

inside end of the torque tube by means of a long stalk (G) running down the bore and the other is fixed to the body of the pressure vessel. The bore of the torque tube is open to the atmosphere so there are no problems of sealing and friction between the stalk and vessel.'

The torque tube is made of fully hardened EN 31 steel (1% Cr 1% C ball race steel) and is designed to be completely elastic at the maximum working pressure. It was calibrated at atmospheric pressure but as the effect of pressure on the shear modulus of the steel is negligible the calibration can be used at all pressures.

In Crossland's original design, the end load due to pressure on the shaft (Q) passing through the Morrison seal (O) was taken by a ball thrust race. This method was unsatisfactory for the higher pressures and the second equalising pressure vessel (A) and seal (O) were added to very nearly completely balance the end load, the remaining end load being taken by the thrust race (T). The Morrison seals give very little friction and a very low leakage rate when they are properly developed and maintained, but they are very sensitive to dirt in the oil and scratches on the mating surfaces. However, the friction in the seals does not affect the experimental results because the torque on the specimen is measured by the torque tube at the other end.

The high pressure fluid surrounding the specimen was the same as that used in the high

pressure intensifier and dead weight pressure tester, namely a 50/50 mixture of castor oil and hydraulic brake fluid. At 7 kbar pure castor oil is much too viscous to be satisfactory. Details of the hollow specimen are shown in fig. 3. It should be noted that the high pressure fluid is in direct contact with the specimen surfaces.

The testing technique consisted of mounting the specimen in the equipment, checking the zero torque reading of the torque bar, pumping the apparatus up to test pressure and leaving it to settle at that pressure for twice as long as the expected duration of the test. The pressure was kept constant by a dead weight pressure tester and the maximum variation of pressure during the test was ± 40 bars. Then the specimen was twisted at a constant rate of strain of the order of $4 \times 10^{-4} \text{ sec}^{-1}$, the torque being noted at regular intervals. Since only the overall twist of the shaft could be measured, very accurate measurements of strain in the gauge length of the specimen were not possible.

3. Results

3.1. Definition

The yield-point is defined as the point of maximum stress on a stress-strain curve which subsequently shows a region of falling stress; the failure of specimens characterised in this way is regarded as ductile. The fracture stress is the stress at failure irrespective of whether the

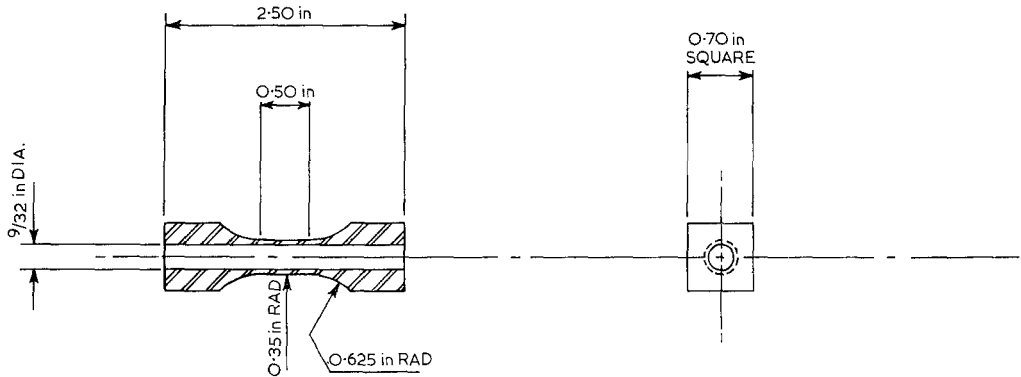


Figure 3 Test specimen.

stress-strain curve shows a maximum. If no maximum is observed the specimen thus described is regarded as brittle.

3.2. General Features

PMMA was examined in the greatest detail and the results are summarised in figs. 4 to 8. The shear stress, τ , is reported as a true stress, calculated from the applied torque and the current second moment of area (corrected to take into account the volume change accompanying pressurisation). The shear strain, ϕ , is based on an effective gauge length for the specimen design shown in fig. 3, and is calculated as

$$\phi = \frac{(\text{outside radius}) \times (\text{angle of twist, radians})}{(\text{effective gauge length})}$$

Fig. 4 illustrates the considerable effect that the application of hydrostatic pressure has on the stress-strain behaviour in torsion of PMMA. Several important features are noted. First, there is a monotonic increase in the initial slope of the stress-strain curve with increasing pressure. This trend is displayed quantitatively in fig. 5 as a plot of shear modulus, G , against applied hydrostatic stress, P . There is also a substantial increase in the yield stress and the strain to yield as the pressure is raised. Further, there is a transition in the mode of failure at elevated pressure, the specimens fracturing in the high pressure region before a drop in stress occurs. Finally, in the high pressure region the fracture stress increases with increasing pressure but the strain of fracture decreases.

Fig. 6 is a plot of the maximum true stress attained in a stress-strain test against the applied hydrostatic pressure. In the range of pressure

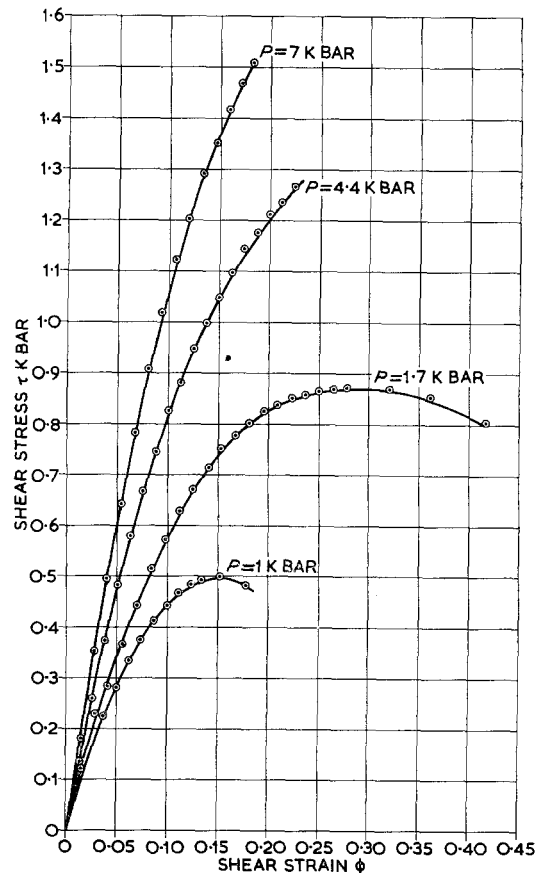


Figure 4 Shear stress-shear strain curves for polymethylmethacrylate at various pressures P .

from one atmosphere to 3.2 kbar the stress-strain curve shows a drop in true stress prior to fracture – the maximum stress is here taken as the yield stress and is seen to vary essentially linearly with hydrostatic stress. As shown in

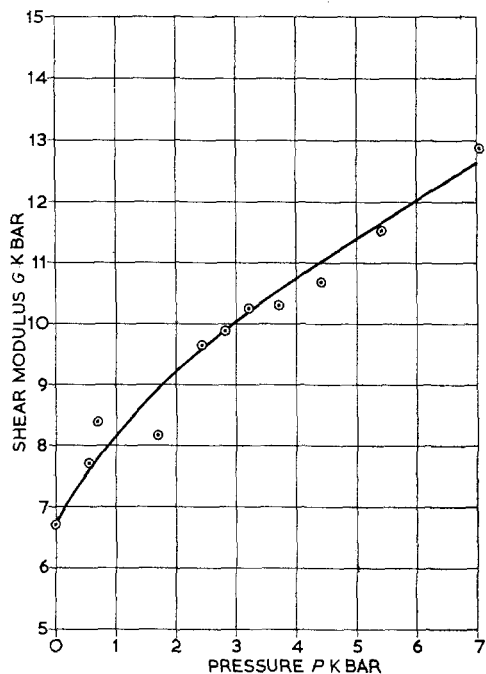


Figure 5 Shear modulus G of polymethylmethacrylate as a function of pressure P .

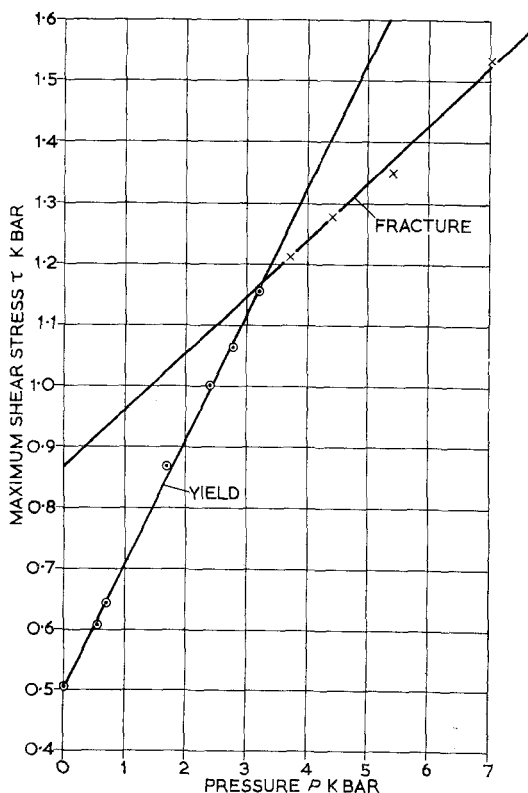


Figure 6 Maximum shear stress τ_y as a function of pressure P for polymethylmethacrylate. \odot , yield; \times , fracture.

fig. 4, fracture closely follows yield in this pressure region; the drop in stress prior to fracture is gradual and small. At applied pressures greater than 3.2 kbar fracture is observed prior to a yield drop. The variation of fracture stress with pressure in this region is also shown in fig. 6. The transition indicated by the intersecting lines in fig. 6 is quite sharp. It was found that tests could be performed such that for 0.25 kbar less than the transition pressure a yield drop was observed, whereas for 0.25 kbar greater than the transition pressure no yield drop occurred.

In describing the yield behaviour of PMMA we have defined the yield point as the maximum true stress. It is important to note, however, that the stress-strain curve shows non-linearity prior to this maximum at all pressures.

Fig. 7 shows the shear stress strain data for all the tests done on PMMA. In many cases two tests were done at the same pressure. The dotted curve showing the envelope of the fracture points illustrates how the strain to fracture at first increases with increase of pressure and then decreases.

The apparent strain at fracture is plotted against hydrostatic stress in fig. 8. It is noted that the fracture strain exhibits a distinct maximum which does not coincide with the pressure for the transition from ductile to brittle failure.

The yield behaviour in the ductile region is summarised in fig. 9 by a series of Mohr-circle plots based on the shear yield stress, τ , and the applied hydrostatic pressure, P . The fracture behaviour in the pressure region (greater than 3.2 kbar) is further illustrated by a plot of σ_F^2/E (σ_F = tensile fracture stress; E = tensile modulus) against hydrostatic pressure in fig. 10.

The data for crystalline poly(ethylene terephthalate) (Arnite type A 150, supplied by BIP Chemicals Ltd) are shown in fig. 11 as shear stress plotted against shear strain for various values of applied pressure. It is noted that the behaviour shown is qualitatively typical of that for the polyethylene samples as well. Fig. 12 is a plot of shear yield stress against pressure for Arnite. Plastic yielding, accompanied by a drop in true stress at yield, was observed over the entire range of pressure. Included in fig. 12 are the results obtained from specimens annealed at 180° C (in air) for 2 h prior to testing. The annealed material fractured in a brittle manner at atmospheric pressure, but was ductile at the lowest applied hydrostatic pressure 0.5 kbar.

The pressure dependence of yield was subsequently indistinguishable from that for the unannealed material.

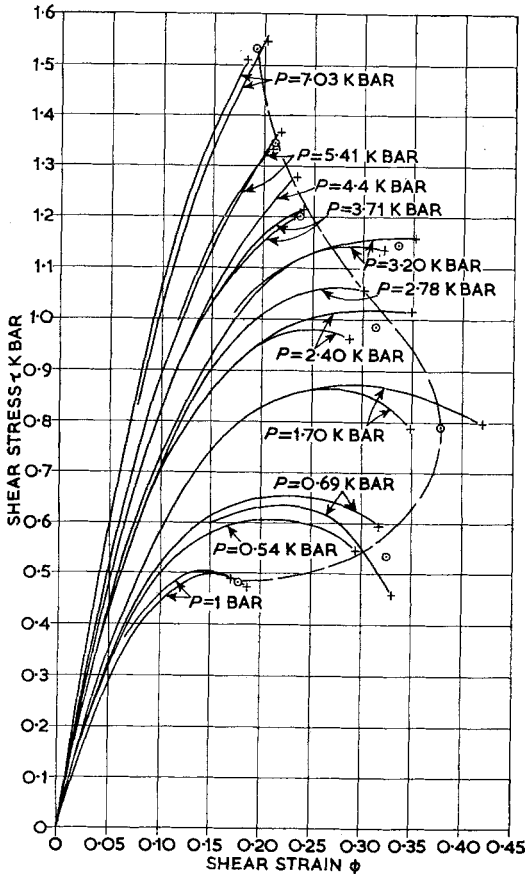


Figure 7 Shear stress-strain curves for polymethylmethacrylate showing fracture envelope.

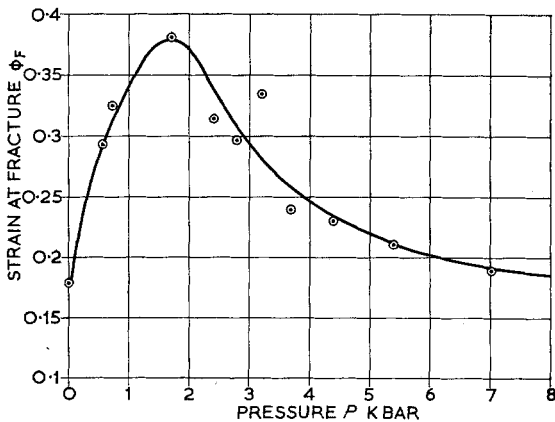


Figure 8 Strain at fracture ϕ_F as a function of pressure P for polymethylmethacrylate.

*1 atm = 101.3 N/m²

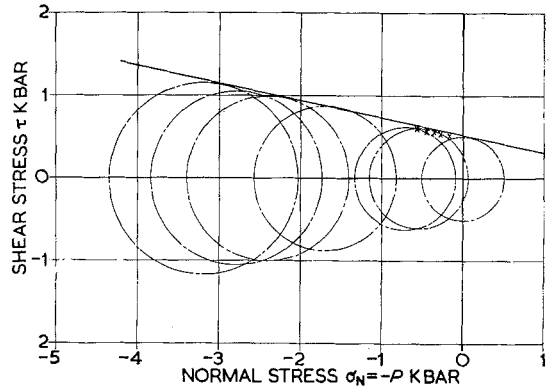


Figure 9 Mohr-circles for yield behaviour of polymethylmethacrylate. The common tangent gives the yield plane at $\sim 30^\circ$.

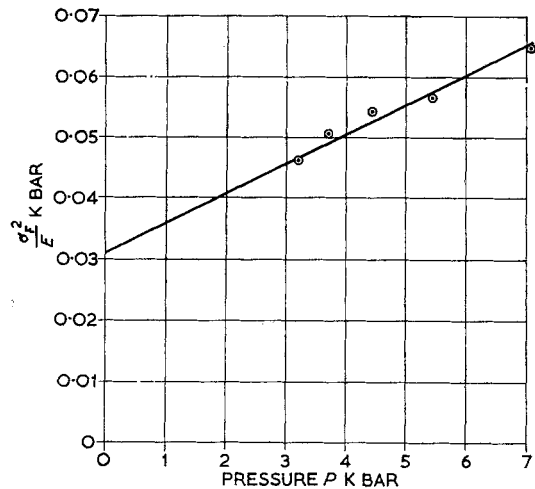


Figure 10 Plot of σ_F^2/E against pressure P for polymethylmethacrylate in the brittle fracture region (σ_F = brittle fracture stress, E = Young's Modulus).

Fig. 13 shows the variation with pressure of the shear yield stress for polyethylene. Polyethylene remained ductile over the complete pressure range, with a pressure dependence of the torsional yield stress which was similar to that shown by polyethylene terephthalate.

Subsidiary experiments were undertaken with PMMA to investigate the possibility of permanent compaction under hydrostatic pressure. After soaking for 2 h at 7 kbar, specimens tested at 1 atm*, 1.7 kbar, and 3.2 kbar revealed stress-strain behaviour identical to that obtained from specimens without pretreatment. The time

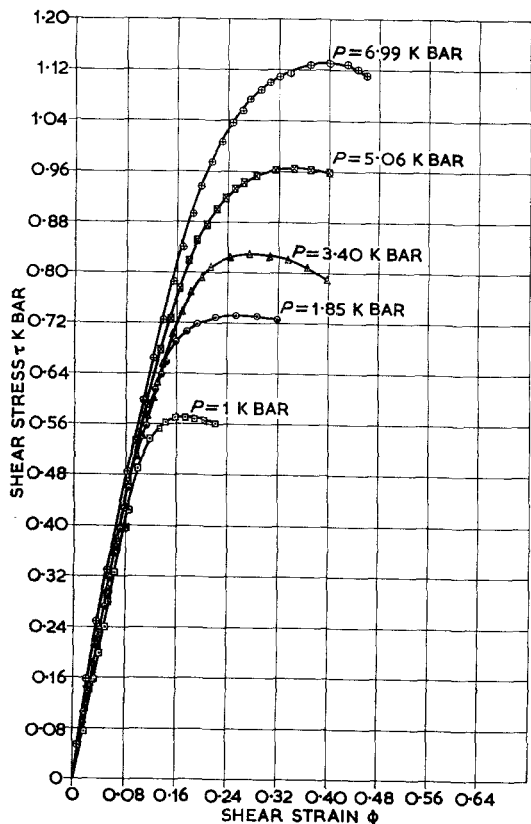


Figure 11 Shear stress-shear strain curves for poly(ethylene terephthalate) at various pressures P .

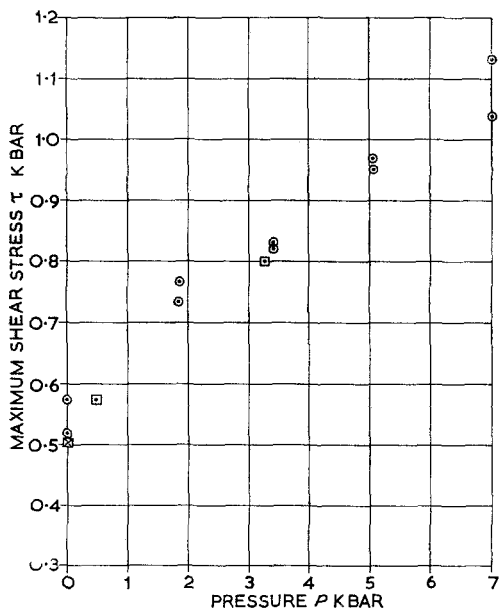


Figure 12 Maximum shear stress as a function of pressure for poly(ethylene terephthalate). \circ , as received; \square , annealed; \bullet , yield; \times , fracture.

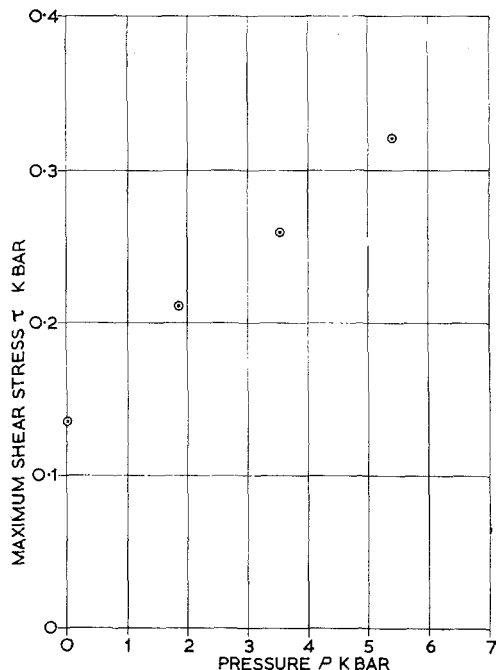


Figure 13 Maximum shear stress as a function of pressure for high molecular weight polyethylene.

for a complete stress-strain test was about 15 min. In addition, the density of the specimens subjected to 7 kbar pressure for 2 h was measured by weighings in air and distilled water and found to be $1.1865 \pm 0.0005 \text{ gm cc}^{-1}$ as compared with $1.1861 \pm 0.0005 \text{ gm cc}^{-1}$ for the untreated material. These results, taken together, indicate that any permanent compaction effects are negligibly small.

4. Discussion

4.1. Pressure Dependence of Shear Modulus

The pressure dependence of the shear modulus of PMMA, shown in fig. 5, amounts to approximately a two-fold increase over a range of 7 kbar pressure. This is considerably less than that reported by Ainbinder *et al* [1], who found a two-fold increase in the *tensile* modulus at a pressure of 2 kbar. Although the torsion testing apparatus here employed does not give an accurate measure of shear modulus, the measurement errors are predominantly systematic and the relative change in shear modulus with pressure is believed to be reliably observed. It is noted that classical elasticity arguments preclude any compatibility between the shear modulus-pressure dependence reported here and

the tensile modulus data in [1]. For consistency, we have converted our observed shear moduli to tensile moduli for use in the analysis of the fracture behaviour (fig. 10); in the absence of reliable Poisson's ratio pressure data, a constant ratio of 0.4 was assumed.

4.2. The Yield Behaviour

The results for the yield behaviour of the three polymers can be represented formally in either of two ways. Firstly, it may be assumed that the hydrostatic component of stress affects the shear stress required to instigate yield. This explanation is one which we favour on physical grounds, and we will show in a further publication that it brings consistency to yield stress measurements made under a variety of different stress fields. Empirically, the PMMA results would be represented by an expression of the form (fig. 6):

$$\tau = \tau_0 + \alpha P \quad (1)$$

where, τ = shear stress yield at pressure P , $\tau_0 = 0.503$ kbar, is the yield stress at atmospheric pressure, and $\alpha = 0.204$ kbar kbar⁻¹, is the coefficient of increase of yield stress with hydrostatic pressure. For crystalline poly(ethylene terephthalate) and polyethylene the dependence of the yield stress on hydrostatic pressure is much less than in PMMA. Fitting the data for these two polymers to the yield criterion of (1), we obtain for Arnite $\tau_0 = 0.575$ kbar, $\alpha = 0.075$ kbar kbar⁻¹; and for polyethylene, $\tau_0 = 0.140$ kbar, $\alpha = 0.034$ kbar kbar⁻¹. These results are consistent with the general conclusions of Ainbinder *et al* [1], that the pressure-dependence of the yield stress of amorphous polymers is greater than that of crystalline polymers. Such behaviour might be expected if, for example, the compressibility of polymers decreased with increasing hydrostatic pressure.

Alternatively, we may describe the yield results in the form of a Coulomb yield criterion, as has been done previously in the case of PMMA by Bowden and Jukes [3] and Whitney and Andrews [2]. The Mohr circle plot in fig. 9 was constructed from the observed combinations of τ and P at yield. The envelope or tangent line of these circles defines the yield criterion as a linear relation between shear yield stress and normal stress on the yield plane; i.e.

$$\tau = \tau_c + \alpha' \sigma_N, \quad (2)$$

where σ_N is the normal stress. For this representation for PMMA we find: $\tau_c = 0.528$ kbar;

$\alpha' = 0.211$ kbar kbar⁻¹, these values to be compared with those previously obtained from (1). The reported data of Bowden and Jukes [3] for PMMA can be fitted into a small part of the plot in fig. 9 and are shown as the crossed points. The corresponding values they obtained were: $\tau_c = 0.474$ kbar, and $\alpha' = 0.158$ kbar kbar⁻¹.

It is interesting to note that the fit to the linear yield stress-pressure dependence of (1) is much better for the amorphous PMMA than for the semicrystalline PET and polyethylene (figs. 6, 12, 13). It will be shown in a further publication that such behaviour may be accounted for by incorporating the pressure-dependence of (1) into a general rate theory for yield in polymers.

4.3. The Fracture Behaviour

The "ductile-brittle" transition at 3.2 kbar provides a convenient demarcation for the discussion of the fracture results of PMMA. At greater pressures, the state of stress and strain at fracture is well defined and the fracture process may be quantitatively evaluated. In the low pressure region, general yielding precedes fracture; here it is difficult to make any more than a qualitative assessment of the fracture behaviour. It is of considerable interest to note that in all but the atmospheric pressure tests fracture occurred when the state of stress in the bulk of the material was wholly compressive, i.e. the hydrostatic component of stress was greater in magnitude than the shear stress at fracture. We have not completely resolved the nature of the fracture process at elevated pressures. *A priori* there are the two possibilities; shear fracture or tensile fracture. These will be discussed in turn.

In order to consider the relative merits of the two fracture modes, it is necessary first to present the results of a cursory topographic analysis of the fractured specimens. Fracture occurred, at all pressures, on planes close to, but deviating somewhat from, 45° to the axis of the cylindrical specimens; i.e. planes of very low shear stress (fig. 14). It is not possible to be more specific because there was an experimental scatter of approximately $\pm 2^\circ$ and, further, because the elastic response of the PMMA specimens was observed with insufficient accuracy to permit a reliable correction for the elastic strain to fracture. There was some indication that the orientation of the fracture plane moved towards 45° to the axis of the cylinder with increasing pressure, but again, the experimental scatter was too great to permit any meaningful analysis.

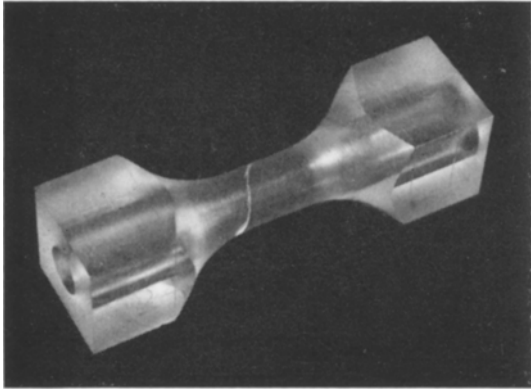


Figure 14 Photograph of fractured specimen.

However, the maximum observed deviation of the fracture plane (in the brittle region) from the 45° direction was about 4.5° . Fracture therefore occurred on planes whose normals lie very close to the direction of maximum tensile stress.

The fracture faces on the hollow cylindrical specimens used for the numerical results were smooth and flat; there was no apparent change in the appearance of the fracture face on going through the "ductile-brittle" transition at 3.2 kbar. Solid cylindrical specimens were fractured for comparative purposes under similar hydrostatic pressures. In the high pressure region the fracture surfaces of the solid specimens showed a region identical in appearance to that of the hollow specimens extending inward from the outer edge a distance greater than the thickness of the hollow specimens. The remainder of the fracture surface was covered with hackle markings. In the low pressure region (below 3.2 kbar) the solid specimens withstood considerably greater strains before fracture; at atmospheric pressure, the strain to fracture of a solid specimen was about 250% as compared with 15% for the hollow specimen geometry. In this region the solid specimens showed a considerable amount of plastic distortion on the fracture surface.

With the above discussion as background, we now consider the possibility that shear fracture is the operative mode of failure. At first sight this assumption is most appealing since the state of stress in the bulk of the specimen at fracture is wholly compressive as long as the applied pressure P is greater in magnitude than the fracture stress τ ; this situation prevails in all but the atmospheric pressure experiment. However, the orientation of the fracture surfaces indicates that fracture is occurring on planes

of almost zero shear stress (and hence, minimum compressive stress). Thus, if shear fracture is occurring it must be governed by a fracture criterion that reflects a compromise between maximising the shear stress and minimising the normal stress on the fracture plane, with the normal stress term(s) dominating the relation overwhelmingly. This hypothesis is rendered highly unlikely by the observation that the mode of fracture is the same at atmospheric pressure and high hydrostatic pressure; i.e. the orientation and appearance of the fracture surface are approximately constant over the full range of pressure. Only the state of stress and strain at fracture changes abruptly at the transition pressure, but the mode of fracture is continuous. At atmospheric pressure, the normal stress on the fracture plane is not compressive but is very nearly the maximum tensile stress generated by the applied shear stress.

The fracture behaviour described above would be much more compatible with tensile fracture initiating at flaws in the surface.

If the hydraulic fluid does not penetrate the flaw or crack, the hydrostatic component of stress will oppose the spreading of the crack and try to close it. On the other hand, should the fluid enter the crack, it will equalise the hydrostatic component of stress and allow the crack to spread.

It is well known that the fracture behaviour of many materials is greatly influenced by whether the hydraulic fluid is in direct contact with the surface of the material [13-16]. In particular, coating metal specimens [16] has been found to inhibit fracture, confirming the proposal that penetration of the hydraulic fluid into surface cracks initiates the fracture process. To test this point it is intended to examine the behaviour of hollow specimens coated with a layer of solidified rubber solution.

We will assume that fracture occurs on planes making an angle of 45° to the axis of the specimen and ignore any component of stress acting along the axis of the specimen. The maximum tensile component of stress, which we will assume is the fracture stress, is then equal to the applied torsional stress at fracture.

It is of interest to examine the fracture strength of PMMA as a function of hydrostatic pressure. The simplest assumption compatible with the data in fig. 6 would be that the fracture stress is linearly dependent on the applied pressure. However, extrapolating the data to

atmospheric pressure (fracture stresses below the transition pressure cannot be directly related to those in the high pressure region because yield precedes fracture in the low pressure range), gives a value for the fracture stress which is much greater than that observed experimentally in tensile fracture tests [17]. In representing the fracture behaviour therefore, we have used a simple argument based on the application of the Griffith theory of fracture [18–20]. On this theory the brittle fracture strength $\sigma_F = \sqrt{(\gamma E/\pi c)}$ for tensile fracture, where γ is the fracture “surface energy”, $E =$ Young’s modulus and c is the length of the intrinsic surface flaw that nucleates the fracture. Both the fracture strength and the Young’s modulus are functions of the applied hydrostatic pressure in the present experiments. We therefore plot σ_F^2/E against P , as shown in fig. 10. This plot suggests that σ_F^2/E , which is proportional to γ , is a linearly increasing function of P (this is why a simpler extrapolation of the fracture behaviour based on the fracture stress alone would not be expected to work). The Griffith theory is constructed on the assumption of brittle fracture, and in that narrow definition γ would represent the surface energy of the growing crack. It is generally well accepted, however, that in PMMA γ reflects almost entirely the energy dissipated in inelastic processes which occur under the high stresses at the crack tip [21]. The variation in γ with pressure would then be expected to correlate with the pressure dependence of the inelastic processes involved in fracture. Consistent with this view, a calculation to determine the contribution to the increase in γ associated with densification of the material under pressure showed that surface energy changes are too small by several orders of magnitude to account for the observed pressure dependence. It is interesting to note that the increase in γ with increasing pressure is similar to its increase with decreasing temperature. In both cases, although the material becomes less ductile (in terms of the strain to fracture) the work done in the fracture process increases. Berry [20] has observed that the same highly deformed surface layer appears on the fracture surface at low temperatures as at higher temperatures. In terms of the decreased segmental mobility of the molecular chains at low temperatures or high pressures it is not surprising that the work done in forming this surface layer increases as the pressure is raised.

*1 dyne = 10^{-5} N.

The data in fig. 10 may be extrapolated to atmospheric pressure to give a set of values for γ , c , and σ_F which are compatible with observations made in tensile fracture experiments on PMMA. We obtain $(\sigma_F^2/E)_{p=0} = 3.5 \times 10^7$ dynes*/cm². Taking $c = 0.25 \times 10^{-2}$ to 0.5×10^{-2} cm, we find $\gamma = 1.4 \times 10^5$ to 2.8×10^5 erg/cm², which is in good agreement with the observations of Berry [20].

In this picture, then, the “ductile-brittle” transition occurs when the yield surface, expanding with increasing pressure, emerges through the more slowly expanding tensile fracture envelope. The same tensile fracture mode is believed to be operative over the entire range of pressure observed, with general plastic yielding preceding fracture at pressures below 3.2 kbar. It is interesting to note that the maximum in the strain to fracture occurs at a hydrostatic pressure considerably below the 3.2 kbar. It is difficult to characterise the state of stress and strain at fracture when yield precedes fracture. It is clear, however, that plastic strain weakens the PMMA in the low pressure region, since here tensile fracture occurs at stress levels well below the nominal tensile fracture stress. Such weakening might occur by the accumulation of damage during plastic deformation. The maximum in the strain to fracture might then arise through the competition of two factors: the increased capacity of the material for plastic deformation (note the increasing strain to yield) and the increasing rate of production of flaws that might nucleate fracture as the current stress at yield increases. It is interesting to point out that similar behaviour has been observed in the rupture of elastomers [21]. With increasing strain rate or decreasing temperature the fracture strength increases steadily but the strain to fracture passes through a maximum value.

4.4. Poly(ethylene Terephthalate)

The Arnite results are somewhat different from those on PMMA. Specimens of Arnite as received from the manufacturer were ductile in torsion at atmospheric pressure, and the torsional yield stress rose monotonically with increasing hydrostatic pressure. Annealing the specimens produced embrittlement at atmospheric pressure, but testing under the lowest measurable pressure (approximately 0.5 kbar) ductile behaviour was observed. Thus we observe that as soon as there is no tensile component of

stress (the applied hydrostatic component of stress more than compensates the tensile component of stress associated with the applied shear stress) the polymer fails in a ductile manner. This behaviour suggests that the brittle behaviour observed at atmospheric pressure is associated with internal flaws produced by the annealing. Such flaws would be impenetrable to the hydraulic fluid. Hence, the application of hydrostatic pressure would result in a large compressive stress resisting separation of the initial crack faces, and brittle fracture would be suppressed.

It is to be noted that although the annealing treatment produces embrittlement at atmospheric pressure, the subsequent yield behaviour under hydrostatic pressure is unaffected (fig. 12). This suggests that whereas the annealing treatment produces internal flaws, it does not significantly modify the microtexture of the polymer, which is perhaps surprising.

Acknowledgement

The authors wish to thank J. B. Watts and F. G. Phillis for their help in collecting the data. One of us (S.R.) is grateful to the National Science Foundation for their support in the form of a Post-doctoral Fellowship in Science.

References

1. S. B. AINBINDER, M. G. LAKA, and I. YU. MAIORS, *Mekhanika Polimerov* **1** (1965) 65.
2. W. WHITNEY and R. D. ANDREWS, *J. Polymer Sci. C16* (1967) 2981.
3. P. B. BOWDEN and J. A. JUKES, *J. Mater. Sci.* **3** (1968) 183.
4. K. D. PAE, D. R. MEARS, and J. A. SAUER, *Polymer Lett.* **6** (1968) 773.
5. G. BIGLIONE, E. BAER, and S. V. RADCLIFFE, Paper presented at Brighton Conference on Fracture (April, 1969).
6. K. D. PAE and D. R. MEARS, *J. Polymer Sci. B6* (1968) 269.
7. L. HOLLIDAY, J. MANN, G. POGANY, H. D. PUGH, and D. A. GREEN, *Nature* **202** (1964) 381.
8. N. BROWN and I. M. WARD, *J. Polymer Sci.* **6** (1968) 607.
9. N. BROWN, R. A. DUCKETT, and I. M. WARD, *Phil. Mag.* **18** (1968) 483.
10. J. M. STEARNE and I. M. WARD, *J. Mater. Sci.* **4** (1969) 1088.
11. B. CROSSLAND, *Proc. IME* **168** (1954) 935.
12. C. M. KAYE, and J. M. ROBERTS, Honours B.Sc. Report No. 68/46 (1968) Mechanical Engineering Dept, University of Bristol.
13. TH. VONKARMAN, *Z. Ver. deutsch. Ing.* **55** (1911) 1749.
14. R. BOKER, Dissertation, Tech. Hochschule zu Aachen, "The Mechanics of Plastic Deformation in Crystalline Bodies".
15. P. W. BRIDGMAN, *J. Appl. Phys.* **18** (1947) 246; "Studies in Large Plastic Flow and Fracture with special emphasis on the effects of hydrostatic pressure" (McGraw-Hill, London and New York, 1952).
16. B. CROSSLAND and W. H. DEARDON, *Proc. IME* **172** (1958) 805.
17. P. BEARDMORE, *Phil. Mag.*, in press.
18. A. A. GRIFFITH, *Phil. Trans.* **221** (1921) 163.
19. J. J. BENBOW and F. C. ROESLER, *Proc. Phys. Soc. B70* (1957) 201.
20. J. P. BERRY, "Fracture Processes in Polymeric Solids" (Wiley, New York, 1964) pp. 195.
21. T. L. SMITH, *J. Polymer Sci.* **32** (1958) 99.

Received 8 September and accepted 6 October, 1969.